

# Nonsingular density profiles of dark matter halos and Strong gravitational lensing

Da-Ming Chen

*National Astronomical Observatories, Chinese Academy of Sciences, Beijing 100012, China*

## ABSTRACT

We use the statistics of strong gravitational lenses to investigate whether mass profiles with a flat density core are supported. The probability for lensing by halos modeled by a nonsingular truncated isothermal sphere (NTIS) with image separations greater than a certain value (ranging from  $0''$  to  $10''$ ) is calculated. NTIS is an analytical model for the postcollapse equilibrium structure of virialized objects derived by Shapiro, Iliev, & Raga. This profile has a soft core and matches quite well with the mass profiles of dark matter-dominated dwarf galaxies deduced from their observed rotation curves. It also agrees well with the NFW (Navarro-Frenk-White) profile at all radii outside of a few NTIS core radii. Unfortunately, comparing the results with those for singular lensing halos (NFW and SIS+NFW) and strong lensing observations, the probabilities for lensing by NTIS halos are far too low. As this result is valid for any other nonsingular density profiles (with a large core radius), we conclude that nonsingular density profiles (with a large core radius) for CDM halos are ruled out by statistics of strong gravitational lenses.

*Subject headings:* cosmology: theory - cosmology: observations - gravitational lensing

## 1. Introduction

The concordant, currently dark energy-dominated, spatially flat cold dark matter (CDM) cosmology is so successful that we are now said to be in an era of “precision cosmology” (Peebles 2002; Ostriker & Souradeep 2004). In this concordant cosmology, dark energy (DE), mainly introduced to close the universe and to explain the accelerating expansion of the universe, attracts much attention in the realms of astrophysics and theoretical physics. The simplest candidate for DE is the cosmological constant, and its more general form, known as quintessence, is a cosmic scalar field minimally coupled with the usual matter (Caldwell,

Dave, & Steinhardt 1998; Ma et al. 1999; Peebles & Ratra 2003). The generalized Chaplygin gas, as a unification of dark matter and dark energy, was recently proposed and can be constrained by observations (Padmanabhan & Choudhury 2002; Zhu 2004). In other cosmological models, DE is replaced by certain possible mechanisms, such as brane world cosmologies (Randall & Sundrum 1999a,b) and the Cardassian expansion model (Freese & Lewis 2002; Zhu & Fujimoto 2002, 2003, 2004). Despite its success, the standard CDM theory of cosmic structure formation has several problems, which exist mostly in the small-scale regime. For example, the observed rotation curves of dark-matter-dominated dwarf and low surface brightness (LSB) disk galaxies tend to favor mass profiles with a flat density core (e.g., Salucci & Burkert 2000; Gentile et al. 2004), unlike the singular profiles of the CDM  $N$ -body simulations (e.g., Navarro, Frenk & White 1997, NFW profiles; Moore et al. 1999; Jing 2000; Jing & Suto 2002) and that favored by baryon cooling models (i.e., singular isothermal sphere, SIS profile). While there are debates on whether the observed data were resolved well enough to indicate a soft core (van den Bosch & Swaters 2001; Marchesini et al. 2002), quite recent  $N$ -body simulations of CDM with higher and higher force and mass resolution still favor cuspy halo profiles (Diemand, Moore & Stadel 2004; Fukushige, Kawai & Makino 2004; Navarro et al. 2004; Tasitsiomi et al. 2004; Wambsganss, Bode & Ostriker 2004).

Recently, an analytical model was presented for the post-collapse equilibrium structure of virialized objects that condense out of a low-density cosmological background universe, with or without a cosmological constant (Shapiro, Iliev & Raga 1999; Iliev & Shapiro 2001). The model is based on the assumption that cosmological halos form from the collapse and virialization of ‘top-hat’ density perturbations, and are spherical, isotropic and isothermal. According to the authors, this predicts a unique, non-singular, truncated isothermal sphere (NTIS) and provides a simple physical clue about the existence of soft cores in halos of cosmological origin. This NTIS model is claimed to be in good agreement with observations of the internal structure of dark matter dominated halos on scales ranging from dwarf galaxies to X-ray clusters. In particular, it matches quite well the mass profiles of dark matter dominated dwarf galaxies deduced from their observed rotation curves (Shapiro et al. 2004). Quite recently, the NTIS model was revisited by using the self-interacting dark matter (SIDM) hypothesis (Ahn & Shapiro 2004). There are other efforts for analytical derivations of the density profile; e.g., Hansen (2004) derived the bound on the central density slope of -1 analytically (as found numerically by NFW). This is done by a simple solution to the Jeans equation, which is valid under the assumption that both the central density profile and the phase-space-like density are exact power laws. However, this work did not clearly give a density core.

To investigate whether there is a soft core at the center of each CDM halo, we use another

independent and robust tool, gravitational lensing, which has been widely used to detect the mass distributions in the Universe (Turner, Ostriker, & Gott 1984; Schneider, Ehlers, & Falco 1992; Wamsgans et al. 1995; Wu 1996; Bartelmann 1996; Wu 2000; Bartelmann & Schneider 2001; Chen 2001; Keeton 2001; Keeton & Madau 2001; Xue & Wu 2001; Keeton 2002, 2003; Pen et al. 2003; Schneider 2003; Keeton & Zabludoff 2004; Wu 2004; Zhang et al. 2004) and the dark energy density and its equation of state (Fukugita, Futamase, & Kasai 1990; Fukugita, & Turner 1991; Turner 1990; Krauss & White 1992; Maoz & Rix 1993; Kochanek 1995, 1996; Falco, Kochanek, & Muñoz 1998; Cooray & Huterer 1999; Waga & Miceli 1999; Sarbu, Rusin, & Ma 2001; Dev, Jain & Alcaniz 2004). Recently, motivated by the current largest homogeneous sample of lensed quasars, coming from the radio Cosmic Lens All-Sky Survey (CLASS; Myers et al. 2003; Browne et al. 2003), an extension of the earlier Jodrell Bank/Very Large Array Astrometric Survey (JVAS; Patnaik et al. 1992; King et al. 1999), much work has been devoted to statistics of strong lensing to constrain the cosmological parameters and mass distribution (Chae et al. 2002; Li & Ostriker 2002; Oguri et al. 2002; Chae 2003; Li & Ostriker 2003; Oguri 2003; Oguri, Suto & Turner 2003; Oguri & Keeton 2004; Wang 2004; Mitchell et al. 2005; Sereno 2005; Zhang et al. 2005). Statistics of strong gravitational lensing by halos with a soft core was studied quite early (Hinshaw & Krauss 1987; Chiba & Yoshii 1999; Cheng & Krauss 2000), but no observational sample suitable for analysis could be used in their work; in particular, they did not use their cored density profile to fit the observed rotation curves of the dwarf and LSB disk galaxies. In strong gravitational lensing of quasars, the separation between multiple images is the most important observable. In some instances, asymmetry and shear of lens halos affect the properties of images considerably, but statistically, image separations are mainly determined by the potential wells of the host halos characterized by the slopes of their density profiles. Thus, the probabilities for lensing by NTIS halos with image separations greater than  $\Delta\theta$  provide us with an independent and powerful probe of the existence of soft cores of CDM halos. Our calculations are performed in a concordant, spatially flat  $\Lambda$ CDM cosmology favored by the *Wilkinson Microwave Anisotropy Probe* (WMAP; Bennett et al. 2003) plus large-scale structure (LSS) data from the Sloan Digital Sky Survey (SDSS; Tegmark et al. 2004a,b), with matter density parameter  $\Omega_m = 0.3$ , galaxy fluctuation amplitude  $\sigma_8 = 0.9$ , and Hubble parameter  $h = 0.72$ . For comparison, we also give the results when NTIS is replaced by SIS+NFW and NFW profiles.

## 2. Lensing Probabilities

In what follows, we use a reduced mass of a halo defined as  $M_{15} = M/(10^{15}h^{-1}M_\odot)$ . The NTIS model is based on the assumption that cosmological halos form from the collapse

and virialization of top-hat density perturbations and are spherical, isotropic, and isothermal (Shapiro, Iliev & Raga 1999; Iliev & Shapiro 2001). The well-fitted density profile is given by (Shapiro, Iliev & Raga 1999; Iliev & Shapiro 2001; Shapiro et al. 2004)

$$\rho(r) = \rho_0 \left( \frac{A}{a^2 + r^2/r_0^2} - \frac{B}{b^2 + r^2/r_0^2} \right), \quad (1)$$

where  $A = 21.38$ ,  $B = 19.81$ ,  $a = 3.01$ , and  $b = 3.28$ . The central value of the density profile is  $\rho_0 = 1.8 \times 10^4 \rho_c(z_{\text{coll}})$ , where  $\rho_c(z_{\text{coll}})$  is the critical density of the Universe at the epoch of halo collapse with redshift  $z_{\text{coll}}$ . The small core radius depends on mass  $M$  and  $z_{\text{coll}}$  and is given by

$$r_0 = 0.115(M/\rho_0)^{1/3} = 6.73 \times 10^{-2} M_{15}^{1/3} [\Omega_m(1 + z_{\text{coll}})^3 + \Omega_\Lambda]^{-1/3} h^{-1} \text{Mpc}, \quad (2)$$

where we have used  $\rho_c(z) = \rho_c(0)[\Omega_m(1 + z)^3 + \Omega_\Lambda]$  (with  $\Omega_m = 0.3$  and  $\Omega_\Lambda = 0.7$  in later calculations) and  $\rho_c(0) = 1.88 \times 10^{-29} h^2 \text{gcm}^{-3} = 2.777 \times 10^{11} h^2 M_\odot \text{Mpc}^{-3}$ . It should be pointed out that the original formula for  $r_0$ , equation (88) in Shapiro et al. (2004), is  $r_0 = 1.51 \times 10^{-3} (M/\rho_0)^{1/3}$  (we write  $M_{200}$  as  $M$ , which is discussed in section 3). This is a clerical error, but we have checked that their subsequent results are not affected by this wrong formula.

The gravitational lens equation is  $\eta = D_S \xi / D_L - D_{LS} \hat{\alpha}$ , where  $\eta$  and  $\xi$  are the physical positions of a source in the source plane and an image in the image plane, respectively,  $\hat{\alpha}$  is the deflection angle, and  $D_L$ ,  $D_S$ , and  $D_{LS}$  are the angular diameter distances from observer to lens, observer to source, and lens to source, respectively. By defining dimensionless positions  $y = D_L \eta / D_S r_0$  and  $x = \xi / r_0$ , and dimensionless angle  $\alpha = D_L D_{LS} \hat{\alpha} / D_S r_0$ , the lens equation is then (Shapiro et al. 2004)

$$y = x - \frac{2ab\kappa_c}{(Ab - Ba)} \left( A\sqrt{a^2 + x^2} - B\sqrt{b^2 + x^2} - Aa + Bb \right), \quad (3)$$

where  $\kappa_c$  is the central convergence:

$$\kappa_c = \frac{\Sigma(\xi = 0)}{\Sigma_{\text{crit}}} = \frac{\pi \rho_0 r_0}{\Sigma_{\text{crit}}} \left( \frac{A}{a} - \frac{B}{b} \right), \quad (4)$$

where  $\Sigma_{\text{crit}} = c^2 D_S / 4\pi G D_L D_{LS}$  is the critical surface density.

It is well known that generally, for any spherically symmetric density profiles of lensing halos, multiple images can be produced only if the central convergence is greater than unity (Schneider, Ehlers, & Falco 1992). When  $\kappa_c \leq 1$ , only one image is produced. Note that even if  $\kappa_c > 1$  is satisfied, multiple images can occur only when the source is located within  $y_{\text{cr}} = y(x_{\text{cr}})$ , where  $x_{\text{cr}}$  is determined from the lensing equation (eq. [3]) with  $dy/dx = 0$

for  $x < 0$  (this is similar to lensing by NFW halos). For a singular density profile such as the SIS and NFW profiles, the central value is divergent, so  $\kappa > 1$  is always satisfied, and multiple images can be produced for any given mass. For density profiles with a finite soft core such as the NTIS profile, however, the condition  $\kappa > 1$  requires that only halos with mass greater than a certain value (determined by  $\kappa_c = 1$ ) can produce multiple images. This is clearly shown in Figure 1, where three curves for  $\kappa_c = 1.1, 1.05$ , and  $1.0$  are plotted, and when  $\kappa_c = 1.0$ , only one image is produced. In lensing statistics, this requirement will limit the populations of lensing halos to quite a small fraction. Such a conclusion is valid for any lensing halos with a finite soft core, which is discussed in detail later.

When quasars at redshift  $z_s$  are lensed by foreground CDM halos of galaxies and clusters of galaxies, the lensing probability for image separations larger than  $\Delta\theta$  is (Turner, Ostriker, & Gott 1984; Schneider, Ehlers, & Falco 1992)

$$P(> \Delta\theta) = \int \mathcal{P}(z_s) dz_s \int_0^{z_s} \frac{dD_L^p(z)}{dz} dz \int_0^\infty \bar{n}(M, z) \sigma(M, z) B(M, z) dM, \quad (5)$$

where  $\mathcal{P}(z_s)$  is the redshift distribution for quasars approximated by a Gaussian model with a mean of 1.27 and a dispersion of 0.95 (Helbig et al. 1999; Marlow et al. 2000; Chae et al. 2002; Myers et al. 2003),  $D_L^p(z)$  is the proper distance from the observer to the lens located at redshift  $z$ ,  $\bar{n}(M, z)$  is the physical number density of virialized dark halos of masses between  $M$  and  $M+dM$ , and  $B(M, z)$  is the magnification bias. The physical number density  $\bar{n}(M, z)$  is related to the comoving number density  $n(M, z)$  by  $\bar{n}(M, z) = n(M, z)(1+z)^3$ ; the latter is originally given by Press & Schechter (1974), and the extended version is  $n(M, z)dM = (\rho_0/M)f(M, z)dM$ , where  $\rho_0$  is the current mean mass density of the universe and

$$f(M, z) = (0.315/M)(d \ln \Delta_z / d \ln M) \exp(-|\ln(\Delta_z/1.68) + 0.61|^{3.8}) \quad (6)$$

is the mass function for which we use the expression given by Jenkins et al. (2001). In this expression,  $\Delta_z = \delta_c(z)/\Delta(M)$ , in which  $\delta_c(z)$  is the overdensity threshold for spherical collapse at redshift  $z$  and  $\Delta(M)$  is the rms of the present variance of the fluctuations in a sphere containing a mean mass  $M$ . The overdensity threshold is given by  $\delta_c(z) = 1.68/D(z)$  for the  $\Lambda$ CDM cosmology (Navarro, Frenk, & White 1997), where  $D(z) = g[\Omega(z)]/[g(\Omega_m)(1+z)]$  is the linear growth function of the density perturbation (Carroll, Press, & Turner 1992), in which  $g(x) = 0.5x(1/70 + 209x/140 - x^2/140 + x^{4/7})^{-1}$  and  $\Omega(z) = \Omega_m(1+z)^3/[1 - \Omega_m + \Omega_m(1+z)^3]$ . When we calculate the variance of the fluctuations  $\Delta^2(M)$ , we use the fitting formulae for the CDM power spectrum  $P(k) = AkT^2(k)$  given by Eisenstein & Hu (1999), where  $A$  is the amplitude normalized to  $\sigma_8 = \Delta(r_M = 8h^{-1}\text{Mpc})$ , given by observations. The cross section for lensing is  $\sigma(M, z) = \pi y_{\text{cr}}^2 r_0^2 \vartheta(M - M_{\text{min}})$ , where  $\vartheta(x)$  is a step function, and  $M_{\text{min}}$  is the minimum mass of halos above which lenses can produce images

with separations greater than  $\Delta\theta$ . The minimum mass  $M_{\min}$  can be derived directly from the relationship between the mass of a lens halo and the corresponding image separation, as follows. It is obvious from Figure 1 that the separation between the outer two images is almost independent of the source position  $y$ . Thus, similar to the analysis for NFW profiles (Li & Ostriker 2002), the image separation  $\Delta x(y)$  produced by a NTIS halo for a source at  $y$  can be well approximated by  $\Delta x(0) = 2x_0$ , where  $x_0$  is the Einstein radius determined from the lens equation with  $y = 0$ . The angular image separation is

$$\Delta\theta = \frac{\Delta x r_0}{D_L} = \frac{2x_0 r_0}{D_L}. \quad (7)$$

Then, from this equation and equation(2) we have

$$M_{\min} = 1.26 \times 10^{12} \left( \frac{1}{x_0} \right) \left( \frac{\Delta\theta}{1''} \right) \left( \frac{D_L}{c/H_0} \right)^3 [\Omega_m(1+z)^3 + \Omega_\Lambda] h^{-1} M_\odot, \quad (8)$$

where  $c/H_0 = 2997.9h^{-1}\text{Mpc}$  is the present Hubble radius. The magnification bias  $B(M, z)$  is calculated numerically with

$$B(M, z) = (2/y_{\text{cr}}) \int_0^{y_{\text{cr}}} dy y [\mu(y)]^{1.1} \quad (9)$$

given by Oguri et al. (2002), where  $\mu(y)$  is the total magnification of the two outer images for a source at  $y$ ; this can also be computed numerically.

The numerical results of Eq. (5) for NTIS lens halos are plotted in figure 2 (*thin solid line*). For comparison, the survey results of JVAS/CLASS and the predicted probability for lensing by SIS + NFW and NFW profiles are also shown. A subset of 8958 sources from the combined JVAS/CLASS survey form a well-defined statistical sample containing 13 multiply imaged sources (lens systems) suitable for analysis of the lens statistics (Myers et al. 2003; Browne et al. 2003; Patnaik et al. 1992; King et al. 1999). The observed lensing probabilities can be easily calculated (Chen 2003b, 2004a) by  $P_{\text{obs}}(> \Delta\theta) = N(> \Delta\theta)/8958$ , where  $N(> \Delta\theta)$  is the number of lenses with separation greater than  $\Delta\theta$  in 13 lenses. The observational probability  $P_{\text{obs}}(> \Delta\theta)$  is plotted as a histogram in Figure 2. In the two-population model SIS + NFW, the galaxy-size and the cluster-size lens halos are approximated by SIS and NFW profiles, respectively (Sarbu, Rusin, & Ma 2001; Li & Ostriker 2002; Chen 2003a,b, 2004a,b; Zhang 2004). In the one-population model NFW, lens halos with different sizes are all approximated by NFW profiles (Li & Ostriker 2002); this is similar to the NTIS model. The theoretically predicted lensing probabilities shown in Figure 2 are calculated separately for three cases (NTIS, SIS+NFW and NFW) according to equation (5). The differences in lensing probability distributions for the three cases arise from their different values for the lensing cross section  $\sigma(M, z)$  and magnification bias  $B(M, z)$ , since these two quantities are

determined uniquely from the corresponding density profile . Here we have recalculated the lensing probabilities for SIS + NFW and NFW profiles according to equation (5). Since the density profiles, lensing equations, and lensing cross sections for SIS and NFW profiles have been discussed many times in the literature, here we only give the final results of lensing probabilities for these two models (for details about SIS+NFW and NFW profiles, see Li & Ostriker 2002; Chen 2004a, and references therein).

### 3. Discussion and Conclusions

One can see clearly from Figure 2 that probability for lensing by NTIS halos with an image separation greater than  $\Delta\theta$  is far too low to match the observational results of CLASS/JVAS; it is even much less than that for NFW lenses. We thus conclude that, at least, NTIS as a model to approximate density profiles of dark matter halos is ruled out by statistical strong lensing. Within the framework of statistics of strong lensing as displayed in the literature, no mechanism can save this model.

In fact the above conclusion is general for any mass profile with a flat soft core characterized by the core density  $\rho_{\text{core}}$  and core radius  $r_{\text{core}}$  (these two parameters are determined by rotation curves of dark matter dominated dwarf and LSB disk galaxies). To see this, we revisit another such density profile, an isothermal sphere with a soft core (cored isothermal sphere, CIS):  $\rho(r) = \sigma_v^2/2\pi G(r^2+r_{\text{core}}^2)$  (Hinshaw & Krauss 1987; Chiba & Yoshii 1999; Cheng & Krauss 2000), where  $\sigma_v$  is the one-dimensional velocity dispersion. The lens equation is

$$y = x - 2\kappa_c^{\text{CIS}}(\sqrt{x^2 + 1} - 1)/x, \quad (10)$$

where  $y$  and  $x$  are defined in the same way as in equation (3) (here  $x = \xi/r_{\text{core}}$ ) and

$$\kappa_c^{\text{CIS}} = \sigma_v^2/2Gr_{\text{core}}\Sigma_{\text{crit}} \quad (11)$$

is the central convergence. Similarly, multiple images can be produced if and only if  $\kappa_c^{\text{CIS}} > 1$ . The corresponding lens equation is plotted in Figure 3 for three different values of  $\kappa_c^{\text{CIS}}$ ; the curves are quite similar to the NTIS model, even though their density profiles seem quite different.

It is not difficult to understand the extremely low value of the probability for lensing by dark halos with a flat soft core. In fact, in our previous calculations, for the NTIS profile,  $\kappa_c$  can be written in the form

$$\kappa_c = 475.7 \frac{\rho_c^{2/3}(z_{\text{coll}})}{\Sigma_{\text{crit}}} M_{200}^{1/3} = 3.65 M_{15}^{1/3} [\Omega_m(1+z)^3 + \Omega_\Lambda]^{2/3} \frac{D_R}{c/H_0}, \quad (12)$$

where  $D_R = D_L D_{LS} / D_s$ . We have defined, as usual, the mass of a dark matter halo to be  $M = M_{200} = 4\pi \int_0^{r_{200}} \rho(r) r^2 dr$  ( $r_{200}$  has its usual definition) and assume that the redshift  $z_{\text{coll}}$  by which the dark halo collapsed is equal to the lens location redshift  $z_L$  and that such an assumption will not affect our results (Shapiro et al. 2004). For a source at  $z_s = 3.0$  and the lens at  $z_L = 0.5$ , equation (12) gives  $\kappa_c = 1.08 M_{15}^{1/3}$ . In this case,  $\kappa_c = 1$  implies  $M \sim M_{15}$ , and this means that for this typical lens system, multiple images can be produced only when the lens mass is higher than  $10^{15} h^{-1} M_\odot$ , which is the typical size of galaxy clusters. By setting  $\kappa_c = 1$  in equation (12), the minimum lens mass for producing multiple images is determined as a function of both  $z_L$  and  $z_s$ . In Figure 4, we plot the mass  $M(\kappa_c = 1)$  (measured in  $M_{15}$ ) as a function of  $z_s$  for three given values of  $z_L$ : 0.1, 0.5, and 1.0. For a given  $z_L$ , the minimum mass decreases with increasing  $z_s$ . Since the mean value of the redshift of the sources is  $\langle z_s \rangle = 1.27$  in our calculations, the actual mean value of the mass for producing multiple images (for lenses at  $z_L = 0.5$ ) is larger than  $10^{15} h^{-1} M_\odot$ . It is also obvious in Figure 4 that in most cases, multiple images can be produced only when the halo mass is larger than  $10^{15} h^{-1} M_\odot$ . From equation (5), we know that the lensing probability is determined by the number density of dark halos and the cross section. As pointed out by Shapiro et al. (2004), an NFW profile would produce more multiple-image lenses than an NTIS one at relatively lower masses, and this trend is reversed at higher masses. Statistically, however, it is the requirement of  $\kappa_c > 1$  and thus the existence of a large core radius that strongly limits the populations of lensing halos [number density  $\bar{n}(M, z)$ ] to quite a small fraction. Thus, the extremely low value of the probability for lensing by NTIS halos arises from the quite low value of the corresponding number density of galaxy clusters. Furthermore, the lensing cross section  $\sigma \sim y_{\text{cr}}^2$ , and from Figure 1 and Figure 3 we see that  $y_{\text{cr}}$  is quite sensitive to  $\Delta\kappa_c = \kappa_c(> 1) - 1$  rather than  $\kappa_c$  itself. Therefore, a slight change in  $\kappa_c \sim M^{1/3}$  will result in a large change both in  $y_{\text{cr}}$  and  $x_0$  (the Einstein radius), and since  $x_0 \sim \Delta\theta$ , this explains the quite flat curve for the NTIS lensing probability in Figure 2 (*thin solid line*). Namely, the insensitivity of NTIS lensing probability to  $\Delta\theta$  reflects the fact that within the image separations of a few arcseconds, the lens mass and thus the corresponding number density of dark halos around that mass change only a little. Similarly, for a CIS profile, after solving the equations

$$M = 800\pi\rho_c r_{200}^3 / 3 \quad (13)$$

$$= 4\pi \int_0^{r_{200}} dr r^2 \sigma_v^2 / 2\pi G (r^2 + r_{\text{core}}^2) \quad (14)$$

$$\approx 2\sigma_v^2 (r_{200} - \pi r_{\text{core}} / 2) / G \quad (15)$$

for  $r_{200}$  and  $\sigma_v^2$ ,  $\kappa_c^{\text{CIS}}$  can be related to dark halo mass  $M$ . The above analysis for the NTIS profile then is also true for the CIS model, if core radius  $r_{\text{core}}$  is large enough to be able to fit the observed rotation curves of the dwarf and LSB disk galaxies.



Note that our conclusion that a CIS model as a cored mass profile is ruled out by statistical strong gravitational lensing seems inconsistent with previous works (Hinshaw & Krauss 1987; Chiba & Yoshii 1999; Cheng & Krauss 2000), since these authors used this model to constrain cosmological parameters. A simple analysis, however, shows us that there is no discrepancy. The central convergence can be expressed in terms of the mass and the core radius of a lens halo. For NTIS, from equation (2) and equation (4), we have  $\kappa_c \propto M/r_0^2$ ; for CIS, from equation (11), equation (13) and equation (15) we have (approximately)  $\kappa_c^{\text{CIS}} \propto M^{2/3}/r_{\text{core}}$ . A larger  $r_{\text{core}}$  needs a larger  $M$  to ensure  $\kappa_c^{\text{CIS}} \geq 1$ , or, for a fixed value of mass  $M$ , an appropriate smaller value of  $r_{\text{core}}$  would ensure  $\kappa_c^{\text{CIS}} \geq 1$ . Therefore, if  $r_{\text{core}}$  is not determined by currently observed rotation curves of the dwarf and LSB disk galaxies, but rather is adjustable (Hinshaw & Krauss 1987; Chiba & Yoshii 1999; Cheng & Krauss 2000), then no discrepancy appears. A more realistic mass profile should not be divergent at the center (cusp), that is, it should have a flat core, but the core radius  $r_{\text{core}}$  should be small enough to ensure that the lensing probability matches the observations of CLASS/JVAS.

I thank the anonymous referee for quite useful suggestions. This work was supported by the National Natural Science Foundation of China under grant 10233040.

## REFERENCES

- Ahn, K., & Shapiro, P. R. 2004, preprint, astro-ph/0412169
- Bennett, C. L., et al. 2003, ApJS, 148, 1
- Bartelmann, M. 1996, A&A, 313, 697
- Bartelmann, M., & Schneider, P. 2001, Phys. Rept., 340, 291
- Browne, I. W. A., et al. 2003, MNRAS, 341, 13
- Caldwell, R. R., Dave, R., & Steinhardt, P. J. 1998, Phys. Rev. Lett., 80, 1582
- Carroll, S. M., Press, W. H., & Turner, E. L. 1992, ARA&A, 30, 499
- Chae, K. -H., et al. 2002, Phys. Rev. Lett., 89, 151301
- Chae, K. -H. 2003, MNRAS, 346, 746
- Chen, D. -M. 2001, Chinese J. Astron. Astrophys., 1, 287

- Chen, D. -M. 2003a, *A&A*, 397, 415
- Chen, D. -M. 2003b, *ApJ*, 587, L55
- Chen, D. -M. 2004a, *A&A*, 418, 387
- Chen, D. -M. 2004b, *Chinese J. Astron. Astrophys.*, 4, 118
- Cheng, Y. -C., & Krauss, L. M. 2000, *Int. J. Mod. Phys. A.*, A15, 697
- Chiba, M., & Yoshii, Y. 1999, *ApJ*, 510, 42
- Cooray, A. R., & Huterer, D. 1999, *ApJ*, 513, L95
- Dev, A., Jain, D., & Alcaniz, J. S. 2004, *A&A*, 417, 847
- Diemand, J., Moore, J., & Stadel, J. 2004, *MNRAS*, 353, 624
- Eisenstein, D. J., & Hu, W. 1999, *ApJ*, 511, 5
- Falco, E. E., Kochanek, C. S., & Muñoz, J. A. 1998, *ApJ*, 494, 47
- Freese, K., & Lewis, M. 2002, *Phys. Lett. B*, 540, 1
- Fukugita, M., Futamase, T., & Kasai, M. 1990, *MNRAS*, 246, 24P
- Fukugita, M., Turner, E. L. 1991, *MNRAS*, 253, 99
- Fukushige, T., Kawai, A., & Makino, J. 2004, *ApJ*, 606, 625
- Gentile, G., Salucci, P., Klein, U., Vergani, D., & Kalberla, P. 2004, *MNRAS*, 351, 903
- Hansen, S. H. 2004, *MNRAS*, 352, L41
- Helbig, P., Marlow, D., Quast, R., Wilkinson, P. N., Browne, I. W. A., & Koopmans, L. V. E. 1999, *A&AS*, 136, 297
- Hinshaw, G. & Krauss, L. M. 1987, *ApJ*, 320, 468
- Iliev, I. T., & Shapiro, P. R. 2001, *MNRAS*, 325, 468
- Jenkins, A., Frenk, C. S., White, S. D. M., Colberg, J. M., Cole, S., Evrard, A. E., Couchman, H. M. P., & Yoshida, N. 2001, *MNRAS*, 321, 372
- Jing, Y. 2000, *ApJ*, 535, 30
- Jing, Y., & Suto, Y. 2002, *ApJ*, 574, 538

- Keeton, C. S. 2001, *ApJ*, 561, 46
- Keeton, C. R. 2002, *ApJ*, 575, L1
- Keeton, C. R. 2003, *ApJ*, 582, 17
- Keeton, C. R., & Madau, P. 2001, *ApJ*, 549, L25
- Keeton, C. R., & Zabludoff, A. I. 2004, *ApJ*, 612, 660
- King, L. J., Browne, I. W. A., Marlow, D. R., Patnaik, A. R., & Wilkinson, P. N. 1999, *MNRAS*, 307, 255
- Kochanek, C. S. 1995, *ApJ*, 453, 545
- Kochanek, C. S. 1996, *ApJ*, 466, 638
- Krauss, L. M., & White, M. 1992, *ApJ*, 394, 385
- Li, L. -X., & Ostriker, J. P. 2002, *ApJ*, 566, 652
- Li, L. -X., & Ostriker, J. P. 2003, *ApJ*, 595, 603
- Ma, C. -P., Caldwell, R. R., Bode, P., & Wang, L. 1999, *ApJ*, 521, L1
- Maoz, D., & Rix, H. -W. 1993, *ApJ*, 416, 425
- Marchesini, D., D’Onghia, E., Chincarini, G., Firmani, C., Conconi, P., Molinari, E., & Zacchei, A. 2002, *ApJ*, 575, 801
- Marlow, D. R., Rusin, D., Jackson, N., Wilkinson, P. N., Browne, I. W. A., & Koopmans, L. 2000, *AJ*, 119, 2629
- Mitchell, J. L., Keeton, C. R., Frieman, J. A., & Sheth, R. K. 2005, *ApJ*, in press (astro-ph/0401138)
- Moore, B., Quinn, T., Governato, F., Stadel, J., & Lake, G. 1999, *MNRAS*, 310, 1147
- Myers, S. T., et al. 2003, *MNRAS*, 341, 1
- Navarro, J. F., et al. 2004, *MNRAS*, 349, 1039
- Navarro, J. F., Frenk, C. S., & White, S. D. M. 1997, *ApJ*, 490, 493
- Oguri, M. 2003, *MNRAS*, 339, L23

- Oguri, M., & Keeton, C. R. 2004, *ApJ*, 610, 663
- Oguri, M., Suto, Y., Turner, E. L. 2003, *ApJ*, 583, 584
- Oguri, M., Taruya, A., Suto, Y., & Turner, E. L. 2002, *ApJ*, 568, 488
- Ostriker, J. P., & Souradeep, T. 2004, *Pramana*, 63, 817
- Padmanabhan, T., & Choudhury, T. R. 2002, *Phys. Rev. D*, 66, 081301
- Patnaik, A. R., Browne, I. W. A., Wilkinson, P. N., & Wrobel, J. M. 1992, *MNRAS*, 254, 655
- Peebles, P. J. E. 2002, preprint, astro-ph/0208037
- Peebles, P. J. E., & Ratra, B. 2003, *Rev.Mod.Phys.*, 75, 559
- Pen, U-L., Zhang, T., van Waerbeke, L., Mellier, Y., Zhang, P., Dubinski, J. 2003, *ApJ*, 592, 664
- Press, W. H., & Schechter, P. 1974, *ApJ*, 187, 425
- Randall, L., & Sundrum, R. 1999a, *Phys. Rev. Lett.*, 83, 3370
- Randall, L., & Sundrum, R. 1999b, *Phys. Rev. Lett.*, 83, 4690
- Salucci, P., & Burkert, A. 2000, *ApJ*, 537, L9
- Sarbu, N., Rusin, D., & Ma, C., -P. 2001, *ApJ*, 561, L147
- Schneider, P., Ehlers, J., & Falco, E. E. 1992, *Gravitational Lenses* (Berlin: Springer-Verlag)
- Schneider, P. 2003, preprint, astro-ph/0306465
- Sereno, M. 2005, *MNRAS*, accepted (astro-ph/0410441)
- Shapiro, P. R., Iliev, I. T., Martel, H., Ahn, K., & Alvarez, M. A. 2004, preprint, astro-ph/0409173
- Shapiro, P. R., Iliev, I. T., & Raga, A. C. 1999, *MNRAS*, 307, 203
- Tasitsiomi, A., Kravtsov, A. V., Gottlober, S., & Klypin, A. A. 2004, *ApJ*, 607, 125
- Tegmark, M., et al. 2004a, *ApJ*, 606, 702
- Tegmark, M., et al. 2004b, *Phys. Rev. D*, 69, 103501

- Turner, E. L. 1990, ApJ, 365, L43
- Turner, E. L., Ostriker, J. P., & Gott, J. R. 1984, ApJ, 284, 1
- van den Bosch, F. R., & Swaters, R. A. 2001, MNRAS, 325, 1017
- Waga, I., & Miceli, A. P. M. R. 1999, Phys. Rev. D, 59, 103507
- Wambsganss, J., Bode, P., Ostriker, J. P. 2004, ApJ, 606, L93
- Wambsganss, J., Cen, R., Ostriker, J. P., & Turner, E. L. 1995, Science, 268, 274
- Wang, J. 2004, Chinese J. Astron. Astrophys., 4, 10
- Wu, X. -P. 2000, MNRAS, 316, 299
- Wu, X. -P. 1996, Fundamentals of Cosmic Physics, 17, 1
- Wu, X. -P. 2004, MNRAS, 349, 816
- Xue, Y. -J., & Wu, X. -P. 2001, ApJ, 549, L21
- Zhang, T. -J. 2004, ApJ, 602, L5
- Zhang, T. -J., Pen, U. -L., Zhang, P.; Dubinski, J. 2004, ApJ, 598, 818
- Zhang, T. -J., Yang, Z. -L., & He, X. -T. 2005, Modern Physics Letters A, 20, 851
- Zhu, Z. -H., & Fujimoto, M. -K. 2002, ApJ, 581, 1
- Zhu, Z. -H., & Fujimoto, M. -K. 2003, ApJ, 585, 52
- Zhu, Z. -H., & Fujimoto, M. -K. 2004, ApJ, 602, 12
- Zhu, Z. -H. 2004, A&A, 423, 421

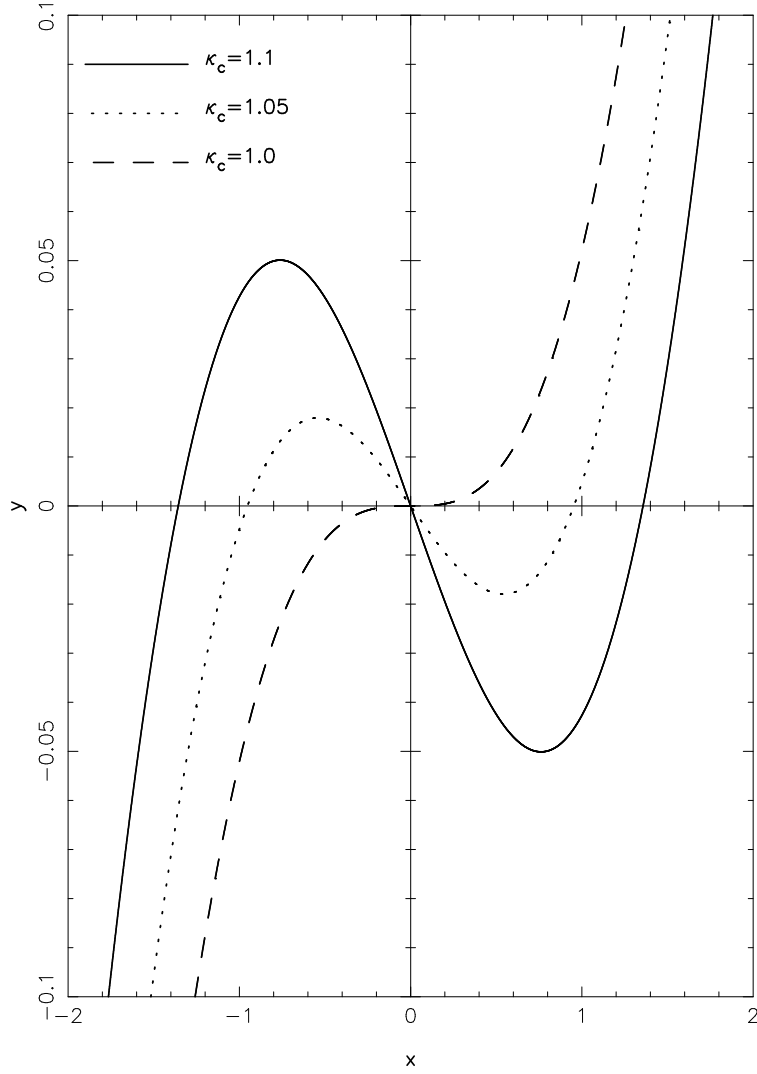


Fig. 1.— Lens equation for NTIS halos, plotted according to equation (3). Coordinates  $y$  and  $x$  are dimensionless positions of the source and the image, respectively. Curves for three values of  $\kappa_c = 1.1$  (*solid curve*), 1.05 (*dotted curve*) and 1.0 (*dashed curve*) are plotted. When  $\kappa_c = 1$ , only one image is created.

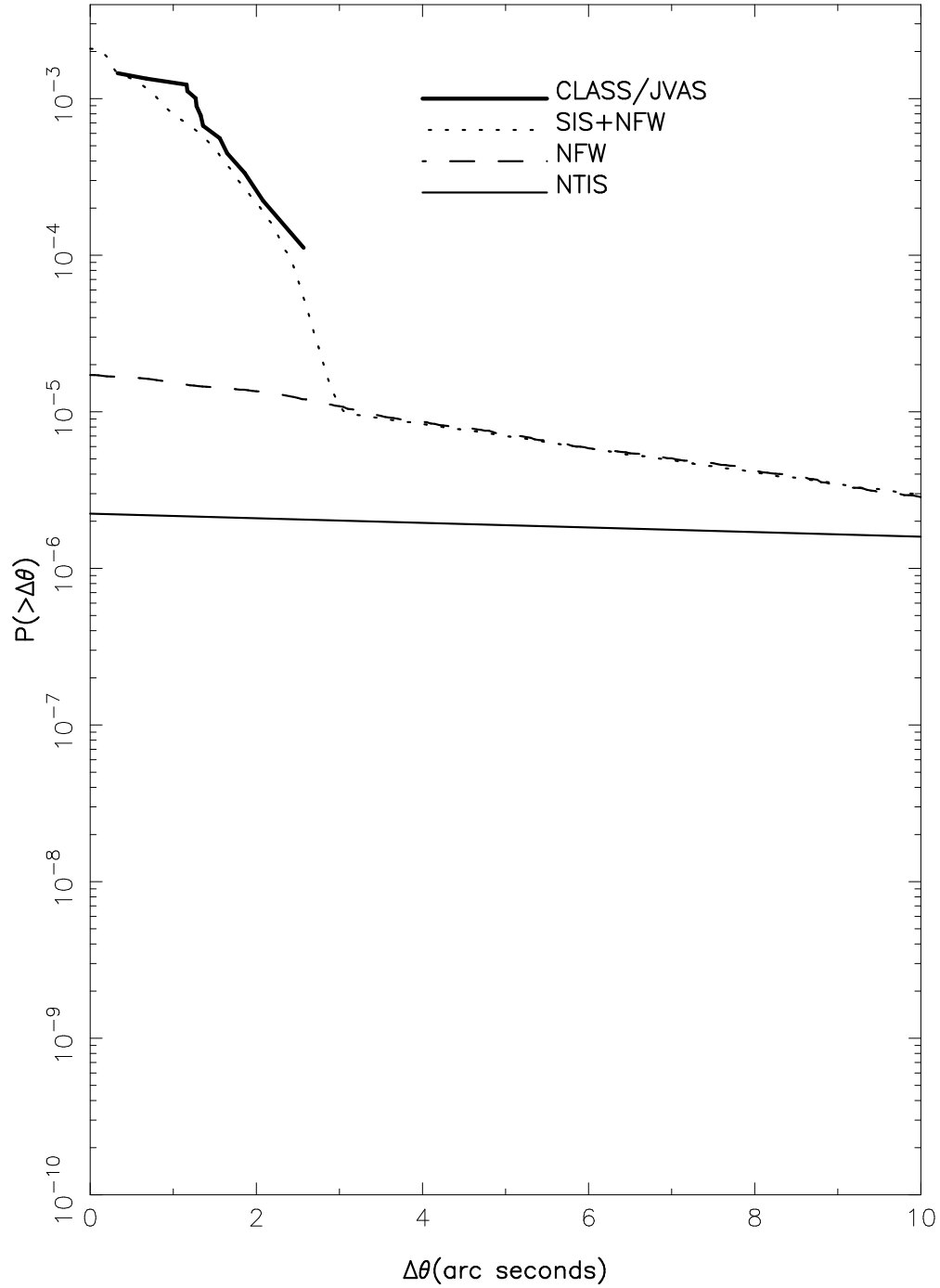


Fig. 2.— Predicted probability for an image separation angle greater than  $\Delta\theta$  for lensing by NTIS halos (*thin solid line*). For comparison, the survey results of JVAS/CLASS (*thick histogram*), the predicted probability for lensing by SIS+NFW (*dotted line*) and NFW (*dashed line*) profiles are also shown.

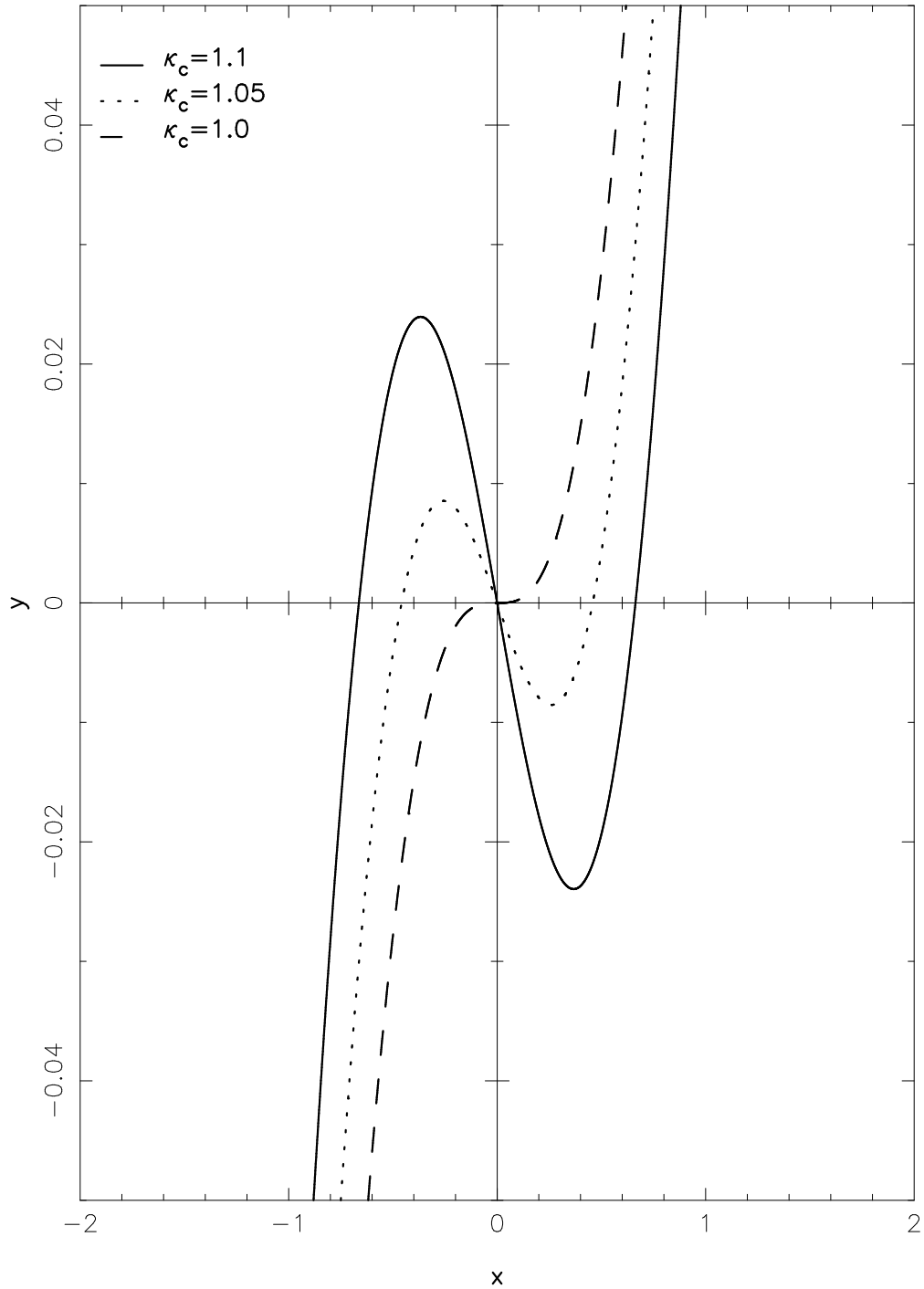


Fig. 3.— Lens equation for CIS halos, plotted according to equation (10). Coordinates  $y$  and  $x$  are dimensionless positions of the source and the image, respectively. Curves for three values of  $\kappa_c = 1.1$  (*solid curve*), 1.05 (*dotted curve*) and 1.0 (*dashed curve*) are plotted. When  $\kappa_c = 1$ , only one image is created.



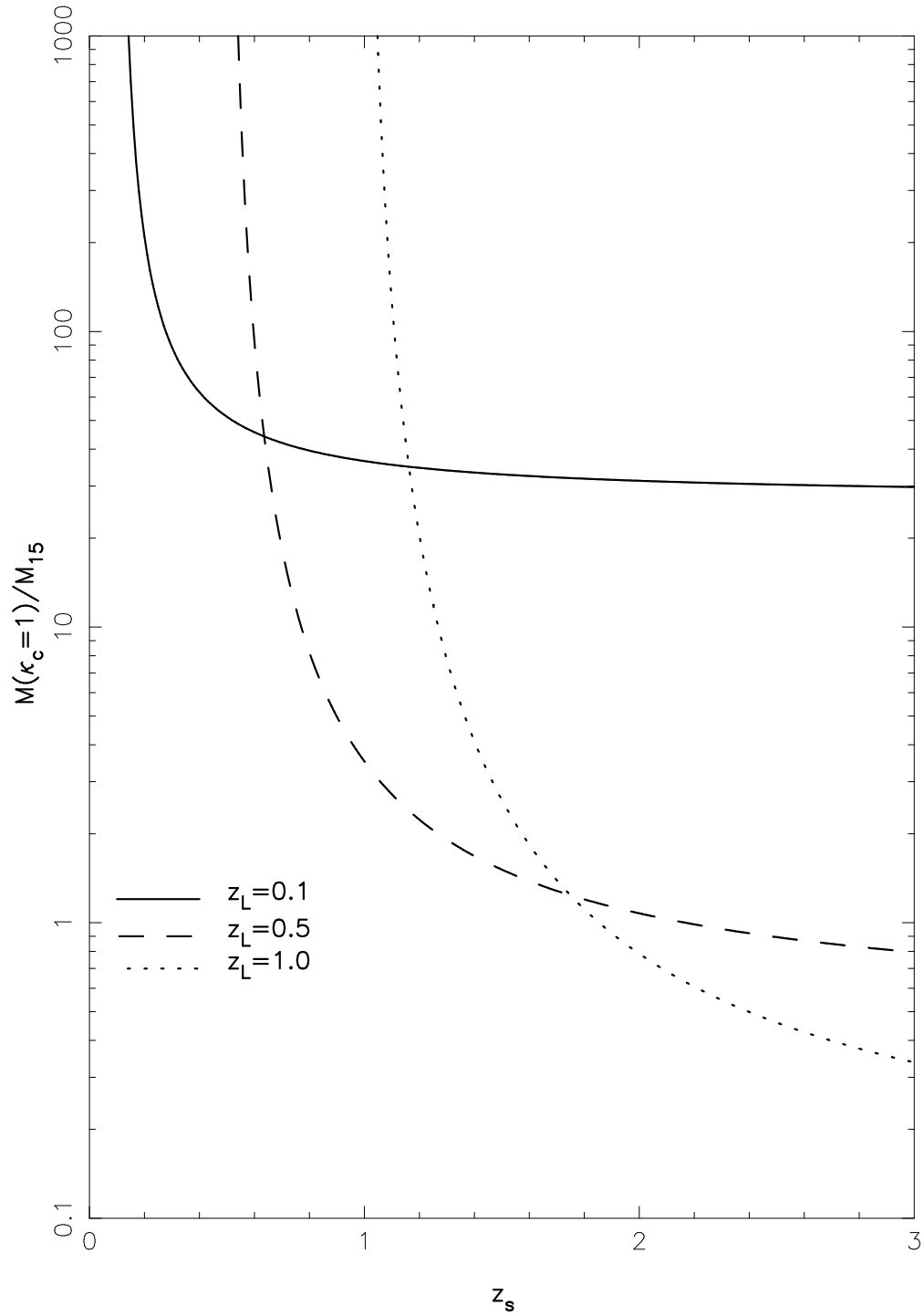


Fig. 4.— Lens mass  $M(\kappa_c = 1)$  as a function of  $z_s$ , determined by setting  $\kappa_c = 1$  in equation (12) for given values of  $z_L$ . Curves for three typical values of  $z_L = 0.1$  (*solid curve*), 0.5 (*dashed curve*) and 1.0 (*dotted curve*) are plotted.